JPET Fast Forward. Published on February 11, 2003 as DOI: 10.1124/jpet.102.047811

JPET/2002/47811

Early Mitochondrial Hyperpolarization and Intracellular Alkalinization in Lactacystin-induced Apoptosis of Retinal Pigment Epithelial Cells

Jong-M. Kim, Hae R. Bae, Bong S. Park, Je M. Lee, Hee B. Ahn, Jee H. Rho, Kyung W. Yoo, Woo C. Park, Sae H. Rho, Hee S. Yoon, and Young Hyun Yoo

Department of Anatomy and Cell Biology (J-.M.K., J.M.L., Y.H.Y.), Department of Physiology (H.R.B.), Department of Ophthalmology (H.B.A., J.H.R., K.W.Y., W.C.P., S.H.R.), Dong-A University College of Medicine and Institute of Medical Science, Busan, South Korea; Department of Oral Anatomy and Cell Biology, Pusan National University, Busan, South Korea (B.S.P.); Sungmo Eye Hospital, Busan, South Korea (H.S.Y.)

Running title: mitochondrial hyperpolarization in RPE cell apoptosis

Corresponding author

Name: Young Hyun Yoo
Address: Department of Anatomy and Cell Biology, Dong-A University College of Medicine, 3-1 Dongdaesin-Dong, Seo-Gu, Busan, South Korea 602-714
Telephone: 82-51-240-2926
Fax: 82-51-241-3767
E-mail: yhyoo@daunet.donga.ac.kr

Number of text pages: 32
Number of tables: 0
Number of figures: 8
Number of References: 39
Number of the words in the Abstract: 244
Number of words in Introduction: 500
Number of words in Discussion: 1131

Recommended section: Cellular and Molecular

Non-standard abbreviations:

SITS; 4-acetamido-4'-isothiocyanostilbene-2,2'-disulphonate

EIPA; 5-N-ethyl-N-isopropyl amiloride

MMP; mitochondrial membrane potential

PVR; proliferative vitreoretinopathy

RPE; retinal pigment epithelial

ABSTRACT

We investigated the induction and underlying mechanism of apoptosis in retinal pigment epithelial cells by the inhibition of proteasome activity using lactacystin. Rat retinal pigment epithelial cell line, RPE-J, was used in this study. Apoptosis was evaluated by light and electron microscopies, DNA electrophoresis and TUNEL assay. The apoptosis-related proteins were localized in the cells by immunofluorescent microscopy, and the changes of their protein contents and the enzyme activation were monitored by Western blot. Mitochondrial membrane potential was quantified by measuring J aggregate (JC-1) fluorescence. To measure changes in intracellular pH, cells were loaded with BCECF and assayed by flow cytometry. To elucidate the type of transport system involving intracellular pH regulation, several transporter inhibitors were employed and their effect on pH and membrane potential was assayed as above. Lactacystin treatment significantly induced apoptosis in RPE-J cells. During the RPE cell apoptosis, i) cytochrome c and Smac/DIABLO were released into cytosol from mitochondria, ii) translocation of AIF to the nucleus was evident, iii) Bax protein appeared to translocate to mitochondria, iv) procaspase-3 and PARP were cleaved, and v) nuclear condensation and DNA fragmentation were clearly observed. Noticeably, a transient increase of mitochondrial membrane potential was coincidentally detected with the intracellular alkalinization after lactacystin administration. Furthermore, the lactacystin-induced early alkalinization was inhibited by 4-acetamido-4'-isothiocyanostilbene-2,2'-disulphonate, an inhibitor of Cl^-/HCO_3^- anion exchanger, which also prevented early mitochondrial hyperpolarization and apoptosis. Lactacystin-induced apoptosis in RPE-J cells is closely associated with an early mitochondrial hyperpolarization induced by intracellular alkalinization.

Introduction

Apoptosis is an evolutionarily conserved, innate process by which cells systemically inactivate, disassemble, and degrade their own structural and functional components to complete their own demise (Wyllie et al., 1980). In this highly regulated process, a cascade of molecular and biochemical events leading to cell death is activated.

Caspase activation is a central process in the execution of dying cells. The activation of an effector caspase, such as caspase-3, is stimulated by activated initiator caspases, caspase-8 or -9. Once activated, the effector caspases are responsible for the proteolytic degradation of a broad spectrum of cellular targets that ultimately leads to cell death (Thornberry and Lazebnik, 1998). However, the activation of effector caspases can be suppressed in the presence of inhibitors of apoptosis proteins (IAPs) (Roberts et al., 2001). Mitochondria play an important role in the regulation of apoptosis. The intermembrane space of mitochondria was proposed to contain several apoptogenic factors [i.e., cytochrome c, procaspases (-2, -3, and –9), and apoptosis inducing factor (AIF)], which are liberated through the outer membrane in order to complete the degradation phase of apoptosis (Green and Reed, 1998; Susin et al, 1999). Smac/DIABLO, a mitochondrial protein that is released from the mitochondria in response to apoptotic stimuli, was found to promote the caspase activation by binding and neutralizing the IAPs (Srinivasula et al., 2000). Bcl-2 family proteins are also well known to enhance (e.g. Bax) or inhibit apoptosis (e.g. Bcl-2, Bcl-xL) (Reed, 1997). Finally, the activation of caspases leads to cleavage of poly(ADP-ribose) polymerase (PARP), degradation of lamins, and endonuclease activation (Thornberry et al, 1997).

Numerous studies have focused on the targeted induction of apoptosis in order to control the unlimited growth of proliferating cells. Retinal pigment epithelial (RPE) cells are thought to contribute significantly to epiretinal membrane formation in proliferative vitreoretinopathy (PVR)

(Machemer and Laqua, 1975; Hiscott and Grierson, 1991; Van Horn et al., 1991). Although in some cases surgery can provide a suitable means of treatment, often it proves futile. Therefore it would be beneficial to pharmacologically inhibit the cellular proliferation. Unfortunately antiproliferative drugs have been toxic and lacked specificity (Khawly et al., 1991). Since it has been previously documented that the growth of proliferative vitreoretinal tissues was regulated in part by the extent of natural cell loss via apoptosis (Esser et al., 1996; Esser et al., 1997), the pharmacological induction of apoptosis in epiretinal membranes could be developed to a new approach to inhibit cellular proliferation in PVR. In this context, we have been seeking the underlying mechanism of RPE cell death (Yoon et al., 2000a and b; Yoon et al., 2001).

In this study, we investigated RPE cell apoptosis by the treatment of proteasome inhibitor, lactacystin, which has been known to induce apoptosis in various cells (Drexler et al., 2000). As will be shown, lactacystin induced apoptosis of RPE-J cells. Importantly, lactacystin-induced apoptosis of RPE-J cells is accompanied by significant increases of mitochondrial membrane potential (MMP) and intracellular pH.

Methods

Reagents

Rabbit polyclonal anti-human PARP antibody was from Oncogene (Cambridge, MA); Rabbit polycolnal anti-horse cytochrome c, anti-mouse Bax and anti-human Bcl-2 and caspase-3, and goat polyclonal anti-mouse AIF antibodies were from Santa Cruz Biotechnology (Santa Cruz, CA). Rabbit anti-mouse Smac/Diablo antibody, a proteasome inhibitor lactacystin, proteasome substrate III Suc-LLVY-AMC (Suc-Leu-Leu-Val-Tyr-aminomethylcoumarine), and multidrug resistance pump inhibitors verapamil and cyclosporin A were from Calbiochem (San Diego, CA). Dulbecco's modified Eagle's medium (DMEM), non-essential amino acids and FCS were from Gibco (Gaithersburg, MD). Pancaspase inhibitior z-VAD-fmk was from Kamiya Biomedical Co. (Seattle, WA). An inhibitor of Cl^-/HCO_3^- anion exchanger 4-acetamido-4'-isothiocyanostilbene-2,2'-disulphonate (SITS), an inhibitor of Na^+/H^+ exchanger 5-N-ethyl-N-isopropyl amiloride (EIPA), nigericin, BCECF-AM and Rhodamine123 were from Molecular Probes (Eugene, OR). Mouse monoclonal anti-β-actin antibody, a F_0F_1-ATPase inhibitor oligomycin, dimethyl sulfoxide (DMSO), RNase A, proteinase K, Poly-L-lysine, aprotinin, leupeptin, and PMSF were from Sigma (St. Louis, MO). ECL western blotting detection reagents were from Amersham International (Buckinghamshire, UK). Mouse monoclonal anti-human Hsp60 antibody was from StressGen Biotechnologies Corp (Victoria, BC Canada).

Cell culture

Retinal pigment epithelial (RPE) cells were purchased from the American Tissue Culture Collection (Rockville, MD). Cells were maintained at 33 °C with 10 % CO_2 in air atmosphere in

DMEM with 4.5 g/L glucose, 2 mM L-glutamine, and 0.1 mM non-essential amino acids supplemented with 4 % FCS. To maintain reproducibility, cells past passage 20 were not used for experiments and early passage cells thawed to renew the culture.

Lactacystin treatment and the effect of caspase inhibitor

Stock solutions of lactacystin (20 mM) made by dissolving the drug in DMSO were kept frozen at –20 °C until use. The concentration of DMSO, 0.05 - 0.25 % (vol/vol), used in this study, both as a vehicle for lactacystin and as a control, had no effect on RPE cell proliferation in our preliminary studies. Twenty four hours after RPE-J cells were subcultured, the original medium was removed. Cells were washed with PBS and then incubated in the same fresh medium. Lactacystin from a stock solution was added to the medium to obtain 10, 20, 30, 40, or 50 μM dilutions of the drug. Since the dose required for half-maximal inhibition of viability at 16 h after lactacystin treatment was about 10 μM, this single concentration was utilized for further assessment of apoptosis of RPE-J cells. In order to study the effect of caspase inhibition, cells were preincubated for 1 h with 100 μM z-VAD-fmk, and then, maintaining the inhibitor in the culture medium, lactacystin was added to obtain 10 μM dilution.

Proteasome activity assay

Cells were lysed in the proteasome buffer, sonicated, and then centrifuged. The supernatant (40 μg of protein) was incubated with proteasome activity buffer [0.005 M Tris-HCl pH 8.0, 0.5 mM EDTA, 50 M Suc-LLVY-AMC] at 37°C for 1h. The intensity of fluorescence was measured by a modular fluorimetric system (Spex Edison, NJ) at 380 nm excitatory and 460 nm emission wavelengths. All readings were standardized using the fluorescence intensity of an equal volume of

free AMC solution (50 μl).

Assessment of cell viability

Cells were released by trypsinization at 16 h after lactacystin treatment, stained with trypan blue and then counted using a hemacytometer.

Morphological Assessment of apoptosis

Light microscopy. Cells were observed and photographed under a phase contrast microscope. Then cells were harvested and cell suspension was centrifuged onto a clean, fat-free glass slide with a cytocentrifuge. Cells were stained in 4 μg/ml Hoechst 33342 for 30 min at 37°C and fixed for 10 minutes in 4% paraformaldehyde. Samples were observed and photographed under an epifluorescence microscope. The number of cells, which showed condensed or fragmented nuclei, was determined by a blinded observer from a random sampling of 250-300 cells per experiment. Four independent experiments were conducted.

Electron microscopy. Cells treated with 10 μM lactacystin for 16 h were collected, centrifuged at 200 x g and fixed in 2.5% glutaldehyde for 1.5 h. The cells were then postfixed in 1% osmic acid for 1.5 h and embedded in epoxy resin. Ultrathin sections were stained with uranyl acetate and lead citrate, and morphological changes were examined using a Hitachi H600-3 electron microscope.

DNA electrophoresis

Cells were harvested 4, 8, 16, 24 and 48 hours after incubation of 10 μM lactacystin. 2×10^6 cells were resuspended in 1.5 ml of lysis buffer [10 mM Tris (pH 7.5), 10 mM EDTA (pH 8.0), 10 mM NaCl and 0.5% SDS］into which proteinase K (200 μg/ml) was added. After samples were

incubated overnight at 48 °C, 200 μl of ice cold 5 M NaCl was added and the supernatant containing fragmented DNA was collected after centrifugation. The DNA was then precipitated overnight at -20 °C in 50% isopropanol and RNase A-treated for 1 h at 37 °C. The DNA from 10^6 cells (15 μl) was equally loaded on each lane of 2% agarose gels in Tris-acetic acid/EDTA buffer containing 0.5 μg/ml ethidium bromide at 50 mA for 2 h.

Immunofluorescent staining

Cells were harvested 4, 8, 16, 24 and 48 hours after incubation of 10 μM lactacystin, and cell suspension was centrifuged onto a clean, fat-free glass slide with a cytocentrifuge. Cytocentrifuged samples were fixed for 10 minutes in 4% paraformaldehyde. Each sample was incubated with each primary antibody for 1 h, washed 3X each for 5 min, and then incubated with FITC-conjugated secondary antibody for 1 h at room temperature. The localization of Bax protein in mitochondria was confirmed by co-localization of mitochondrial protein, HSP-60, using a double immunofluorescence method. Cells were observed and photographed under an epifluorescence microscope. The number of cells, which had lost the punctate staining pattern for cytochrome c, was counted as above.

Western blot analysis for Bcl-2, Bax, PARP or caspase-3

For antibody cleavage blots, 2×10^6 cells treated with 10 μM lactacystin were washed twice with ice-cold PBS, resuspended in 200 μl ice-cold solubilizing buffer [300 mM NaCl, 50 mM Tris-Cl (pH 7.6), 0.5% TritonX-100, 2 mM PMSF, 2 μl/ml aprotinin and 2 μl/ml leupeptin] and incubated at 4 °C for 30 min. The lysates were centrifuged at 14,000 rpm for 15 min at 4 °C and SDS and Na-DOC (final concentration 0.2%, respectively) were added. Protein concentrations of

cell lysates were determined by the method of Bradford (Bio-Rad protein assay) and 50 μg of proteins were loaded onto 12% SDS/PAGE. The gels were transferred to a PVDF membrane (Amersham) and reacted with anti-Bcl-2, anti-Bax, anti-PARP and anti-caspase-3 antibodies. Immunostaining with antibodies was performed using ECL western blotting reagents and detected by LAS-1000Plus (Fujifilm, Japan). β-actin was used for the control.

MMP

Changes in MMP 4, 8, 16, 24 and 48h after treatment with lactacystin (10 μM) were determined by staining cells with the indicator dye, 5,5',6,6'-tetrachloro-1,1',3,3'-tetraethylbenzimidazol carbocyanine iodide (JC-1). JC-1 was added directly to the cell culture medium (1 μM final concentration) and incubated for 15 min. The medium was then replaced with PBS, and cells were quantified for JC-1 aggregated fluorescence intensity in a modular fluorimetric system (Spex Edison, NJ) using excitation and emission filters of 492 and 590 nm. To demonstrate alterations in J-aggregate morphologically, cells incubated with JC-1 were dropped on the microscopic slide, and observed and photographed under an epifluorescence microscope. In addition, MMP was also measured by flow cytometry. Cells were resuspended in 10 μg/ml of methanol and incubated at 37 °C for 30 min. Flow cytometry was performed on a Epics XL (Beckman Coulter, FL, USA). Data were acquired and analyzed using EXPO32 ADC XL 4 color software. The analyzer threshold was adjusted on the FSC channel to exclude noise and most of the subcellular debris.

Intracellular pH measurements

Cells were centrifuged immediately after sampling from the culture, washed in DMEM, and centrifuged again. The cells were then resuspended in 1ml of DMEM, and the pH sensitive dye

BCECE-AM was added to a final concentration of 1 μM from a stock solution of 1 mM in DMSO. The suspension was incubated for 30 min at 33 °C and agitated occasionally to prevent cell settling. BCECF loaded cells were washed twice with ice cold PBS and kept on ice until analysis by flow cytometry. A pH calibration curve was generated by preloading cells with 1 μM BCECF-AM followed by incubation for 30 min in a high-[K+] buffer at different pH values from 6.0 to 8.0 with 0.5 unit increments in the presence of K^+/H^+ ionophore (1 μM). The high-[K+] buffer were obtained by mixing appropriate portions of two buffers containing 135 mM KH_2PO_4, 20 mM NaCl and 110 mM K_2HPO4, 20 mM NaCl, respectively.

For the inhibition of pH regulating system, cells were treated with 100 μM SITS, 100 μM EIPA or 5 μg/ml oligomycin in combination with 10 μM lactacystin for 4 h. The changes of intracellular pH and MMP were measured simultaneously using both BCECF and JC-1. To investigate the effect of these inhibitors on apoptosis, 24 h after treatments induction of apoptosis was assessed by Hoechst staining.

Statistical analysis

Statistical results were expressed as the mean ± the standard deviation of the means obtained from each independent experiment. The results of the experimental and control groups were tested for statistical significance by a one-tailed Student's *t* test or a two-tailed ANOVA.

Results

Lactacystin decreased RPE-J cell viability

Lactacystin treatment caused a significant decrease in the viability of RPE-J cells, dose-dependently, and optimally 10 μM of lactacystin concentration showed about a 50 % of the cell death at 16 hr after treatment (Fig. 1). Proteasome activity decreased very rapidly from 10 min after lactacystin treatment ($p<0.01$) and remained unchanged until 48 h of the same culture (Fig. 2).

RPE-J cells showed typical manifestations of apoptosis after lactacystin treatment

Oligonucleosomal DNA fragmentation, hallmark of apoptosis, was also detected in the DNA from lactacystin-treated cells at 8 – 48 h during the culture (Fig. 3A). Light microscopy after staining the cells with Hoechst 33342 dye revealed apoptosis of RPE-J cells exposed to lactacystin (10 μM). Whereas the round nuclei were observed in the control cells, lactacystin-treated RPE-J cells displayed fragmented or atypical shrunken nuclei (Fig. 3B). Furthermore, electron microscopic study showed that lactacystin-treated cells have condensation of nuclear poles. On the contrary, RPE-J cells in control retained the extensive microvilli and a nucleus with evenly dispersed nuclear chromatin. The cytoplasm of some treated-cells contained several nuclear fragments (Fig. 3C).

Lactacystin-induced apoptosis of RPE-J cells was mediated by caspase-3

Western blotting study showed that lactacystin treatment caused caspase-3 activation. As shown in

figure 4A, the lactacystin induced cleavage of procaspase-3 (p32) into the processed caspase-3 p20 product. Additionally, in lactacystin-treated cells, degradation of intact PARP (116 kD) to 85 kD form of PARP was clearly appeared at 8 h when the caspase-3 activation was detectable (Fig. 4A). Moreover, in the presence of caspase inhibitor, zVAD-fmk, caspase-3 activation and PARP cleavage were evidently suppressed (Fig. 4B), and the nuclear condensation was also prevented (Fig. 4C).

Mitochondrial events were involved in lactacystin-induced apoptosis of RPE-J cells

The changes in protein expression levels of Bax and Bcl-2 were monitored by Western blot. Although Bcl-2 levels decreased gradually after lactacystin treatment, Bax level was only increased transiently at 8 h (Fig. 5A). Immunofluorescent staining showed that Bax was concentrated with a punctate pattern after treatment of lactacystin, which assumed that Bax had translocated into mitochondria (Fig. 5B). Releases of several mitochondrial apoptogenic factors were also observed. Whereas cytochrome c was localized in mitochondria with a punctate pattern in the control cells, it showed a diffuse distribution in the lactacystin-treated cells. Quantitatively, the release of mitochondrial cytochrome c into cytosol increased in a time-dependent manner after lactacystin treatment (Fig. 5C). The translocations of AIF to nucleus and Smac/DIABLO to the cytosol were also demonstrated by their immunofluoresence in the cells (Fig. 5D&E). However, MMP, which reduces commonly in apoptotic process, sustained in the increased levels over the time period of 16 h after lactacystin treatment and thereafter it reduced (Fig. 6A). To exclude the misleading results, alterations in cellular accumulation of JC-1 are assayed in the absence and presence of the inhibitor of mitochondrial multidrug resistance pump. Results showed that both verapamil (50 μg/ml) and cyclosporin A (20 μg/ml) did not influence on the lactacystin-induced change of JC-1 fluorescence

(data not shown). We also presented alterations of MMP by fluorescent microphotographs (Fig. 6B). JC-1 formed the characteristic J-aggregates in the mitochondria of control cells. Compared to that of control cells, the fluorescence intensity from J-aggregate of treated cells increased over the time period of 16 h after treatment, and thereafter it reduced.

Early mitochondrial hyperpolarization in lactacystin-induced apoptosis of RPE-J cells is caused by intracellular alkalinization mediated by Cl^-/HCO_3^- anion exchanger

The correlation of mitochondrial hyperpolarization and change of intracellular pH was studied. Cytosolic pH at various time points after lactacyctin treatment was measured using the pH indicator BCECF. Intracellular pH rose above pH 8.0 following lactacystin addition, with a peak at 16 h. Afterwards intracellular pH decreased down below pH 6.0 at 24 – 48 h, which is indicative of complete death of cells. Interestingly, an additional peak at pH 6.3 appeared after 16 h incubation of lactacystin, implicating that some population of cells had already entered the stage of late apoptosis and subsequent cell death. The initial rise of intracellular pH after lactacystin treatment followed the parallel to the time course of increase in mitochondrial potential (Fig. 7A). To elucidate the ion transport system involving intracellular pH regulation in this type of apoptosis, the effect of several transporter inhibitors on the intracellular alkalinization was further studied. The rise of intracellular pH to 8.0 at 4 h treatment of lactacystin was completely blocked in the presence of 100 μM SITS, an inhibitor of Na^+-independent Cl^-/HCO_3^- anion exchanger (Fig. 7B). However, lactacystin-induced early alkalinization was not prevented either by inhibition of Na^+/H^+ exchanger by 100 μM EIPA or by inhibition of mitochondrial F_0F_1-ATPase by 5 μg/ml oligomycin. To test whether intracellular alkalinization induces mitochondrial hyperpolarization, we next investigated that prevention of early

alkalinization could inhibit mitochondrial hyperpolarization. The blockade of intracellular alkalinization by 100 μM SITS completely abolished the effect of lactacystin to hyperpolarize MMP (Fig. 8A). EIPA, which did not inhibit the intracellular alkalinization, failed to block the rise of mitochondrial potential induced by lactacystin. However, oligomycin by itself did have effects not only to decrease resting MMP but also to inhibit lactacystin-induced mitochondrial hyperpolarization.

We further investigated what influence these early changes in cytosolic alkalinization and mitochondrial hyperpolarization have on eventual apoptosis. In the presence of SITS the later intracellular acidification was also delayed and more cells survived after 24 h lactacystin treatment (Fig. 8B). On the contrary, both EIPA and oligomycin, which did not have inhibitory effects on early intracellular alkalinization, rather accelerated the later acidification and increased the number of dead cells after 24 h lactacystin treatment. These results suggest that early prevention of lactacystin-induced alkalinization delays the progression into terminal acidification and apoptosis.

Discussion

The ubiquitin-proteasome system, which is a fundamental nonlysosomal machinery for degradation of short-lived proteins in the cells, has been known to be involved in apoptosis (Drexler et al., 2000; Orlowski, 1999; Drexler, 1997; Meng et al., 1999). Not only some studies demonstrated that apoptotic stimuli induced apoptosis by inhibiting the proteasome activity of the target cell (Meng et al., 1999), but others reported that proteasome inhibitor itself induced apoptosis in a certain cell (Drexler et al., 2000). In the past several years, there have been rapid progresses in understanding the regulation and mechanisms of apoptosis induced by proteasome inhibition. Recent studies have demonstrated that the proteasome-mediated step(s) in apoptosis generally locate upstream of mitochondrial changes and caspase activation. In addition, inhibition of the proteasome activity caused a suppression of NF-κB activation (Delic et al., 1998) as well as accumulation of Bax protein to mitochondria/cytoplasm (Li and Dou, 2000). The present study demonstrated for the first time that lactacystin induced apoptosis of RPE cells. We have shown that lactacystin treatment caused the RPE-J cell death by apoptotic fashion with the involvement of Bax, AIF, Smac/DIABLO and caspase-3.

On the other hand, the ubiquitin-proteasome system has been empathized as an attractive target in proliferative disease therapy (Delic et al., 1998; Orlowski et al., 1998; Adams et al., 1999; Lin et al., 1998). Several studies showed that proteasome inhibitor prevented the proliferation of cancer cells *in vivo* as well as *in vitro* (Orlowski et al., 1998; Adams et al., 1999). Proteasome inhibitor was also able to increase the antiproliferative effect of certain drugs and to prevent the development of resistance to teniposide induced by brefeldin A (Lin et al., 1998). In addition, proteasome inhibitor sensitized chemo- and radio-resistant cancers to TNFα-induced apoptosis (Delic et al., 1998). The

synergistic antitumor effect of proteasome inhibitor and other antiproliferative agents was also shown *in vivo* (Golab et al., 2000). Therefore, proteasome inhibitor as a single or in combination with a certain antiproliferative drug has become a promising therapeutic strategy (Delic et al., 1998; Lin et al., 1998; Golab et al., 2000). Although the lactacystin seemingly reduced the viability of primary neuronal cells *in vitro* (data not shown), the potential application of lactacystin as a therapeutics for the treatment of PVR still cannot be excluded without further investigations. In the present study, we have found that the lactacystin effectively induced RPE cell death *in vitro* with the concentrations from 10 μM up to 50 μM which could be useful data for its pharmacological application in PVR *in vivo*.

Since the alterations in mitochondrial structure and function play a key role in the regulation of apoptosis (Kroemer et al., 1997; Green and Reed, 1998), it has been generally accepted that changes in mitochondrial membrane integrity precede apoptotic death. Cytochrome c release and disruption of MMP are in fact known features in apoptosis triggered by proteasome inhibition (Marshansky et al., 2001; Wagenknecht et al., 2000). The reduction of MMP was also evidently observed in our previous study on genistein-induced apoptosis of RPE cells (Yoon et al., 2000a). However, it was noteworthy that the early transient mitochondrial hyperpolarization before reduction of MMP was observed in the present study. In few previous studies of apoptosis, early mitochondrial hyperpolarization was described (Green and Reed, 1998; Marzo et al., 1998; Vander Heiden et al., 1997; Li et al., 1999). A research group observed that a form of mitochondrial hyperpolarization shortly preceded the late events of swelling and rupture of the outer membrane (18 h after cytokine withdrawal), and they attributed it to the energy of the proton gradient not being dissipated by ATP synthesis, producing a hyperpolarized state (Marzo et al., 1998). Another group reported that Bcl-X_L countered this process (Green and Reed, 1998; Vander Heiden et al., 1997). A more recent study of

p53-induced apoptosis demonstrated that the generation of ROS led to a transient increase in $\Delta\Psi m$ after induction of p53 expression, just preceding mitochondrial depolarization (Li et al., 1999). However, the precise mechanism(s) involved in mitochondrial hyperpolarization is still unclear. It is quite possible that different mechanisms (both permeability transition-dependent and –independent) may be operating in different experimental systems, or at different time points. Furthermore, particular care should be exerted in studies of MMP with fluorescent probes (Bernardi et al., 1999). The most important problem with the vast majority probes for MMP is that their cellular accumulation can be drastically reduced because of efficient extrusion by the MDR. Moreover, there is a report that cyanine derivative JC-1 appears to be not a ratio-metric probe for MMP (Bernardi et al., 1999). However, we in this study employed JC-1 with a method that is well established by a leading research group of mitochondrial hyperpolarization (Khaled et al., 2001a).

Recent studies depicted the involvement of a rise of intracellular pH in mitochondrial hyperpolarization in the type of apoptosis induced by cytokine withdrawal (Khaled et al., 2001a and b; Khaled et al., 1999; Belaud-Rotureau et al., 2000). Therefore, we have aimed to show whether mitochondrial hyperpolarization observed in lactacystin-induced apoptosis of RPE cell is evoked by cytosolic alkalization. In this study we demonstrated for the first time that SITS-sensitive Na-independent Cl^-/HCO_3^- exchanger mediated a transient rise of intracellular pH induced by lactacystin and that blockade of cytosolic alkalinization prevented mitochondrial potential to rise. However, mitochondrial F_1F_o-ATPase inhibitor oligomycin that inhibited mitochondrial hyperpolarization did not affect intracellular alkalinization. In general, our findings support the idea that a rise in intracellular pH induces mitochondrial hyperpolarization, which is quite similar with the findings of cytokine withdrawal-induced apoptosis in thymocytes and pro-B-cells (Khaled et al., 2001a). In our system, mitochondrial hyperpolarization appears to be mediated by oligomycin-

sensitive mitochondrial F_1F_o-ATPase. However, the fact that blockade of mitochondrial hyperpolarization did not prevent intracellular alkalinization reversely also supports the idea that the intracellular alkalinization precedes and induces mitochondrial hyperpolarization. A rise in intracellular pH is known to inactivate the inhibitory protein (IF1) of the mitochondrial F_1F_o-ATPase complex, which might account for mitochondrial hyperpolarization (Khaled et al.,1999).

Recently, the significance of intracellular alkalinization in apoptosis has been suggested (Khaled et al., 2001; Belaud-Rotureau et al., 2000). The rise in intracellular pH activates Bax and that Bax activation leads to mitochondrial dysfunction in ceramide- (Belaud-Rotureau et al., 2000), cytokine withdrawal- (Khaled et al., 2001a), and TNF-α- (Tafani et al., 2002) induced apoptosis. A precise relationship between the rise in intracellular pH and Bax activation is not demonstrated in the present study, however, it would be important to explore a mechanism(s) underlying RPE-J cell apoptosis by the proteosome inhibitor.

In conclusion, we have demonstrated that the treatment of lactacystin, evokes intracellular alkalinization, which, in turn, might result in apoptosis of RPE-J cells via the mitochondrial hyperpolarization.

References

Adams J, Palombella VJ, Sausville EA, Johnson J, Destree A, Lazarus DD, Maas J, Pien CS, Prakash S, and Elliott PJ. Proteasome inhibitors: a novel class of potent and effective antitumor agents (1999) *Cancer Res* **59:**2615-2622.

Belaud-Rotureau MA, Leducq N, Macouillard Poulletier de Gannes F, Diolez P, Lacoste L, Lacombe F, Bernard P, and Belloc F. Early transitory rise in intracellular pH leads to Bax conformation change during ceramide-induced apoptosis (2000). *Apoptosis* **5:**551-560.

Bernardi P, Scorrano L, Colonna R, Petronilli V, and Di Lisa F (1999) Mitochondria and cell death. Mechanistic aspects and methodological issues. Eur J Biochem **264:**687-701.

Delic J, Masdehors P, Omura S, Cosset JM, Dumont J, Binet JL, and Magdelenat H (1998) The proteasome inhibitor lactacystin induces apoptosis and sensitizes chemo- and radioresistant human chronic lymphocytic leukaemia lymphocytes to TNF-alpha-initiated apoptosis. *Br J Cancer* **77:**1103-1107.

Drexler HC, Risau W, and Konerding MA. Inhibition of proteasome function induces programmed cell death in proliferating endothelial cells (2000). *FASEB J* **14:**65-77.

Drexler HCA. Activation of the cell death programm by inhibiton of proteasome function (1997) *Proc Natl Acad Sci USA* **94:**855-860.

Esser P, Bartz-Schmidt KU, Walter P, Kaszli F, Heimann K, and Weller M. Apoptotic cell death in proliferative vitreoretinopathy (1996) *Ger J Ophthalmol* **5:**73-78.

Esser P, Heimann K, Bartz-schmidt KU, Fontana A, Schraermeyer U, Thumann G, and Weller M. Apoptosis in proliferative vitreoretinal disorders: possible involvement of TGF-β-induced RPE cell apoptosis (1997). *Exp Cell Re.***65:**365-378.

Golab J, Stoklosa T, Czajka A, Dabrowska A, Jakobisiak M, Zagozdzon R, Wojcik C, Marczak M, and Wilk S (2000) Synergistic antitumor effects of a selective proteasome inhibitor and TNF in mice. *Anticancer Res* **20:**1717-1721.

Green DR and Reed JC. Mitochondria and apoptosis (1998) *Science* **281:**1309-1312.

Hiscott PS and Grierson I. Subretinal membranes of proliferative vitreoretinopathy (1991) *Br J Ophthalmol* **75:**53-64.

Khaled AR, Kim K, Hofmeister R, Thompson CB, Muegge K, and Durum SK. Withdrawal of IL-7 induces Bax translocation from cytosol to mitochondria through a rise in intracellular pH (1999). *Proc Natl Acad Sci USA* **96:**14476-14481.

Khaled AR, Moor AN, Li A, Kim K, Ferris DK, Muegge K, Fisher RJ, Fliegel L, and Durum SK. Trophic factor withdrawal: p38 mitogen-activated protein kinase activates NHE1, which induces intracellular alkalinization (2001) *Mol Cell Biol* **21:**7545-7557.

Khaled AR, Reynolds DA, Young HA, Thompson CB, Muegge K, and Durum SK (2001) Interleukin-3 withdrawal induces an early increase in MMP unrelated to the Bcl-2 family. *J Biol Chem* **276:**6453-6462.

Khawly JA, Saloupis P, Hatchell DL, and Machemer R (1991) Daunorubicin treatment in a refined experimental model of proliferative vitreoretinopathy. *Graefe's Arc Clin Exp Ophthalmol* **229:**464-467.

Li B and Dou QP. Bax degradation by the ubiquitin/proteasome-dependent pathway: involvement in tumor survival and progression (2000) *Pro Natl Acad Sci USA* **97:**3850-3855.

Li PF, Dietz R, and von Harsdorf R (1999) p53 regulates mitochondrial membrane potential through reactive oxygen species and induces cytochrome c-independent apoptosis blocked by Bcl-2. *EMBO J* **18:**6027-6036.

Lin ZP, Boller YC, Amer SM, Russell RL, Pacelli KA, Patierno SR, and Kennedy K (1998) A. Prevention of brefeldin A-induced resistance to teniposide by the proteasome inhibitor MG-132: involvement of NF-kappaB activation in drug resistance. *Cancer Res* **58:**3059-3065.

Machemer R and Laqua H. Pigment epithelium proliferation in retinal detachment (massive periretinal proliferation) (1975) *Am J Ophthalmol* **80:**1-23.

Marshansky V, Wang X, Bertrand R, Luo H, Duguid W, Chinnadurai G, Kanaan N, Vu MD, and Wu J (2001) Proteasomes modulate balance among proapoptotic and antiapoptotic Bcl-2 family members and compromise functioning of the electron transport chain in leukemic cells. *J Immunol* **166:**3130-3142.

Marzo I, Brenner C, Zamzami N, Jurgensmeier JM, Susin SA, Vieira HL, Prevost MC, Xie Z, Matsuyama S, Reed JC, and Kroemer G (1998) Bax and adenine nucleotide translocator cooperate in the mitochondrial control of apoptosis. *Science* **281:**2027-2031.

Meng L, Kwok BH, Sin N, and Crews CM (1999) Eponemycin exerts its antitumor effect through the inhibition of proteasome function. *Cancer Res* **59:**2798-2801.

Orlowski RZ, Eswara JR, Lafond-Walker A, Grever MR, Orlowski M, and Dang CV (1998) Tumor growth inhibition induced in a murine model of human Burkitt's lymphoma by a proteasome inhibitor. *Cancer Res* **58:**4342-4348.

Orlowski RZ (1999) The role of the ubiquintin-proteasome pathway in apoptosis. *Cell Death Differ* **6:**303-313.

Reed JC (1997) Double identity for proteins of the Bcl-2 family. *Nature* **387:**773-776.

Roberts DL, Merrison W, MacFarlane M, and Cohen GM (2001) The inhibitor of apoptosis protein-binding domain of Smac is not essential for its proapoptotic activity. *J Cell Biol* **153:**221-228.

Srinivasula SM, Datta P, Fan XJ, Fernandes-Alnemri T, Huang Z and Alnemri ES (2000) Molecular

determinants of the caspase-promoting activity of Smac/DIABLO and its role in the death receptor pathway. *J Biol Chem* **275:**36152-36157.

Steinhorst UH, Chen EP, Hatchell DL, Samsa GP, Saloupis PT, Westendorf J, and Machemer R (1993) Aclacinomycin A in the treatment of experimental proliferative vitreoretinopathy. *Invest Ophthalmol Vis Sci* **34:**1753-1760.

Susin SA, Lorenzo HK, Zamzami N, Marzo I, Snow BE, Brothers GM, Mangion J, Jacotot E, Costantini P, Loeffler M, Larochette N, Goodlett DR, Aebersold R, Siderovski DP, Penninger JM, and Kroemer G (1999) Molecular characterization of mitochondrial apoptosis-inducing factor. *Nature* **397:** 441-446.

Tafani M, Cohn JA, Karpinich NO, Rothman RJ, Russo MA, Farber JL (2002) Regulation of Intracellular pH Mediates Bax Activation in HeLa Cells Treated with Staurosporine or Tumor Necrosis Factor-alpha. *J Biol Chem* **277**:49569-49576.

Thornberry NA and Lazebnik Y (1998) Caspases. Enemies within. *Science* **281:**1312-1316.

Thornberry NA, Rosen A, and Nicholson DW (1997) Control of apoptosis by proteases. *Adv Pharmacol* **41:**155-177.

Van Horn DL, Aaberg TM, and Machemer R (1991) Glial cell proliferation in human retinal detachment with massive preretinal proliferation. *Am J Ophthalmol* **84:**383-393.

Vander Heiden MG, Chandel NS, Williamson EK, Schumacker PT, and Thompson CB (1997) Bcl-xL regulates the membrane potential and volume homeostasis of mitochondria. *Cell* **91:**627-637.

Wagenknecht B, Hermisson M, Groscurth P, Liston P, Krammer PH, and Weller M (2000) Proteasome inhibitor-induced apoptosis of glioma cells involves the processing of multiple caspases and cytochrome c release. *J Neurochem* **75:**2288-2297.

Wyllie AH, Kerr FFR, and Currie AR (1980) Cell death: The significance of apoptosis. *Int Rev Cytol*

68:251-306.

Yoon HS, Moon SC, Kim ND, Park BS, Jeong MH, and Yoo YH. Genistein induces apoptosis of RPE-J cells by opening mitochondrial PTP (2000) *Biochem Biophy Res Commun* **276:**151-156.

Yoon HS, Rho JH, Yoo KW, Park WC, Rho SH, Choi YH, Suh H, Kim ND, Yoo KS, and Yoo YH (2001) Synthetic bile acid derivatives induced nonapoptotic death of human retinal pigment epithelial cells. *Curr Eye Res* **22:**367-374.

Yoon HS, Roh SH, Jeong JH, Yoon S, Yoo KS, and Yoo YH (2000) Effect of genistein on RPE-J cells: Genistein produces reduction in growth and induces apoptosis. *Curr Eye Res* **20:**215-224.

Fig. 1. Effect of lactacystin treatment on viability of RPE-J cells as determined by trypan blue dye exclusion. The cells incubated with different lactacystin concentrations (0-50 μM) for 16 hours were stained with trypan blue dye and then counted using a hemacytometer. Lactacystin produced a dose-dependent decrease in the viability of RPE-J cells ($p<0.01$, 0 – 30 μM). Four independent assays were performed and data shown are the mean ± SD of the means obtained from triplicates of each experiment. Analyzed by two-tailed ANOVA test.

Fig. 2. Time course proteasome activity assay in RPE-J cells after 10 μM lactacystin treatment. After incubation with proteasome activity buffer, the intensity of fluorescence was measured by a modular fluorimetric system. Proteasome activity decreased after lactacystin treatment ($p<0.01$, 5 - 10 min), and thereafter remained the decreased level until 48 h. Data are expressed as the percent of control. Four independent assays were performed and data shown are the mean ± SD of the means obtained from triplicates of each experiment. Analyzed by two-tailed ANOVA test.

Fig. 3. Evaluation of apoptosis in RPE-J cells treated with 10 μM lactacystin for 16 h. The control group was treated with the same concentration of DMSO except lactacystin. (A) DNA fragmentation analysis on the agarose gel electrophoresis. Cells treated with lactatcystin show DNA degradation characteristic of apoptosis with a ladder pattern of DNA fragments. (B) Hoechst 33342 staining. Whereas the control cells have the typical round nuclei (a), cells treated with lactacystin show fragmented atypical nuclei (b). Bar, 40 μm. (C) Electron micrographs. A representative control cell (a) exhibits the typical RPE-J cell morphology which includes microvilli and a nucleus containing evenly distributed nuclear chromatin. A representative early apoptotic cell (b) shows the disappearance of surface folds and condensation of nucleus (arrows). An apoptotic body is demonstrated. In the cytoplasm, several fragmented nuclei are shown, which represents late apoptosis (c). Bar, 4 μm.

Fig. 4. Involvement of caspase-3 in 10 μM lactacystin-induced apoptosis in RPE-J cells. (A) Western blot showing caspase-3 and PARP activations. Lactacystin induced caspase-3 and PARP degradations, and produced the processed caspase-3 p20 and PARP p85 cleavage products. (B) Western blot showing the effect of caspase inhibitor zVAD-fmk on caspase-3 and PARP activations. Control cells were vehicle-treated, experimental cells were treated only with 10 μM lactacystin (L), or 10 μM lactacystin and 100 μM zVAD-fmk (L+Z) for 16 h. zVAD-fmk inhibited caspase-3 and PARP activations. (C) Quantification of apoptotic cells after Hoechst staining. zVAD.fmk (L+Z) prevented nuclear condensation compared to the lactacystin only-treated group (L). *, $p<0.05$. **, $p<0.01$. Four independent assays were performed and data shown are the mean ± SD of the means obtained from triplicates of each experiment. Analyzed by one-tailed Student's *t* test.

Fig. 5. Involvement of mitochondrial events in 10 μM lactacystin-induced apoptosis in RPE-J cells. (A) Western blotting analysis of Bcl-2 and Bax at various time points. (B) Immunofluorescent micrographs showing localization of Bax and Western blot of Bax from cytosolic and mitochondrial fractions. While the control cells show a diffuse distribution (a). the cells 8 h after treatment show a punctate pattern (b). Translocation of Bax into mitochondria can be confirmed by a double staining of HSP-60 in the same sample (c). A scale bar, 20 μm. (C) Cytochrome c localization and Western blot of cytochrome C from mitochondrial and cytosolic fractions. Immunofluorescent micrographs show that vehicle-treated control cells show a punctate pattern (a), whereas cells 8 h after treatment show a diffuse distribution (b). (D) Immunofluorescent micrographs showing localization of AIF. Control cells show punctate pattern (a), whereas lactacystin-treated cells show cytoplasmic staining (c). (b) shows Hoecsht 33258 staining nuclear morphology. (E) Immunofluorescent micrographs showing localization of Smac/DIABLO and Western blot of Smac/DIABLO from mitochondrial and cytosolic fractions. Control cells show punctate pattern (a), whereas lactacystin-treated cells show diffused fluorescence in the cytoplasm or nucleus (b). A scale bar in (E) indicates 40 μm for C-E.

Fig. 6. Mitochondrial membrane potential and JC-1 fluorescence features of mitochondria in RPE-J cells after lactacystin treatment. MMP ($\Delta\Psi m$) at various time points after 10 μM lactacystin treatment. $\Delta\Psi m$ sustained in the increased levels over the time period of 16h, and thereafter decreased ($p<0.01$). Four independent assays were performed and data shown are the mean ± SD of the means obtained from triplicates of each experiment. Analyzed by two-tailed ANOVA test. Microphotographs show JC-1 fluorescence at various time points (0 – 48 h). Data shown are a representative of four independent experiments. A scale bar, 40 μm.

Fig. 7. Histograms displaying lactacystin-induced intracellular alkalinization. (A) RPE-J cells were treated with 10 μM lactacystin for various time points. Cells were then stained with 1 μM BCECF and assayed by flow cytometry. For the pH calibration, cells were exposed 1 μM nigericin in a high-$[K^+]$ buffer at different pH values from 6.0 to 8.0. Cytosolic pH rose transiently up to pH 8.0 until 16 h after lactacystin treatment and fell down below pH 6.0 afterwards. An additional peak at pH 6.3 appeared after 16 h incubation of lactacystin. Four independent experiments were performed. (B) RPE-J cells were treated with 100 μM 4-acetamido-4'-isothiocyanostilbene-2,2'-disulphonate (SITS), 100 μM 5-N-ethyl-N-isopropyl amiloride (EIPA) or 5μg/ml oligomycin (OL) in the presence of 10 μM lactacystin for 16 h. Intracellular pH was measured by flow cytometry using BCECF. Lactacystin-induced early intracellular alkalinization was blocked by SITS but not by EIPA or oligomycin. Five independent experiments were performed.

Fig. 8. Effects of transporter inhibitors on lactacystin-induced mitochondrial hyperpolarization and apoptosis. (A) RPE-J cells were treated with 100 μM 4-acetamido-4'-isothiocyanostilbene-2,2'-disulphonate (SITS), 100 μM 5-N-ethyl-N-isopropyl amiloride (EIPA) or 5μg/ml oligomycin in the presence or absence of 10 μM lactacystin. MMP ($\Delta\Psi m$) at 4 h was measured by JC-1 aggregated fluorescence intensity. Note that inhibition of intracellular alkalinization by 100 μM SITS completely abolished lactacystin-induced mitochondrial hyperpolarization ($p>0.05$). Four independent experiments were performed. (B) RPE-J cells were treated same as above and the viability of RPE-J cells at 24 h was determined by trypan blue dye exclusion. In combination treatment group with SITS and lactacystin, the viability was increased but it decreased in combination treatment group with EIPA or oligomycin compared to the lactacystin only treatment group (**, $p<0.01$). Five independent experiments were performed. Analyzed by one-tailed Student's *t* test.

Fig.1

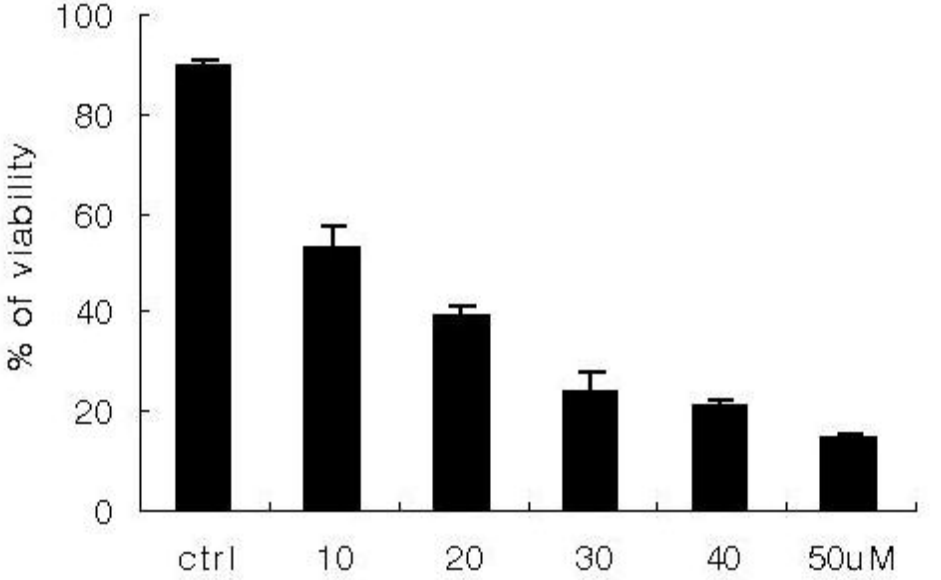

Fig.2

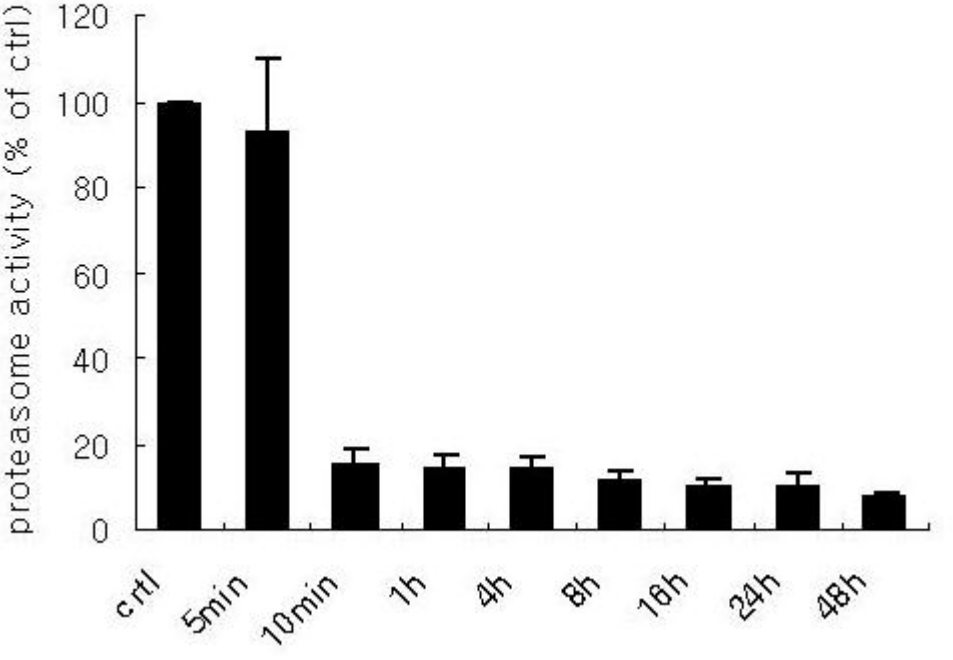
proteasome activity (% of ctrl)
120
100
80
60
40
20
0
ctrl
5min
10min
1h
4h
8h
16h
24h
48h

Fig.3

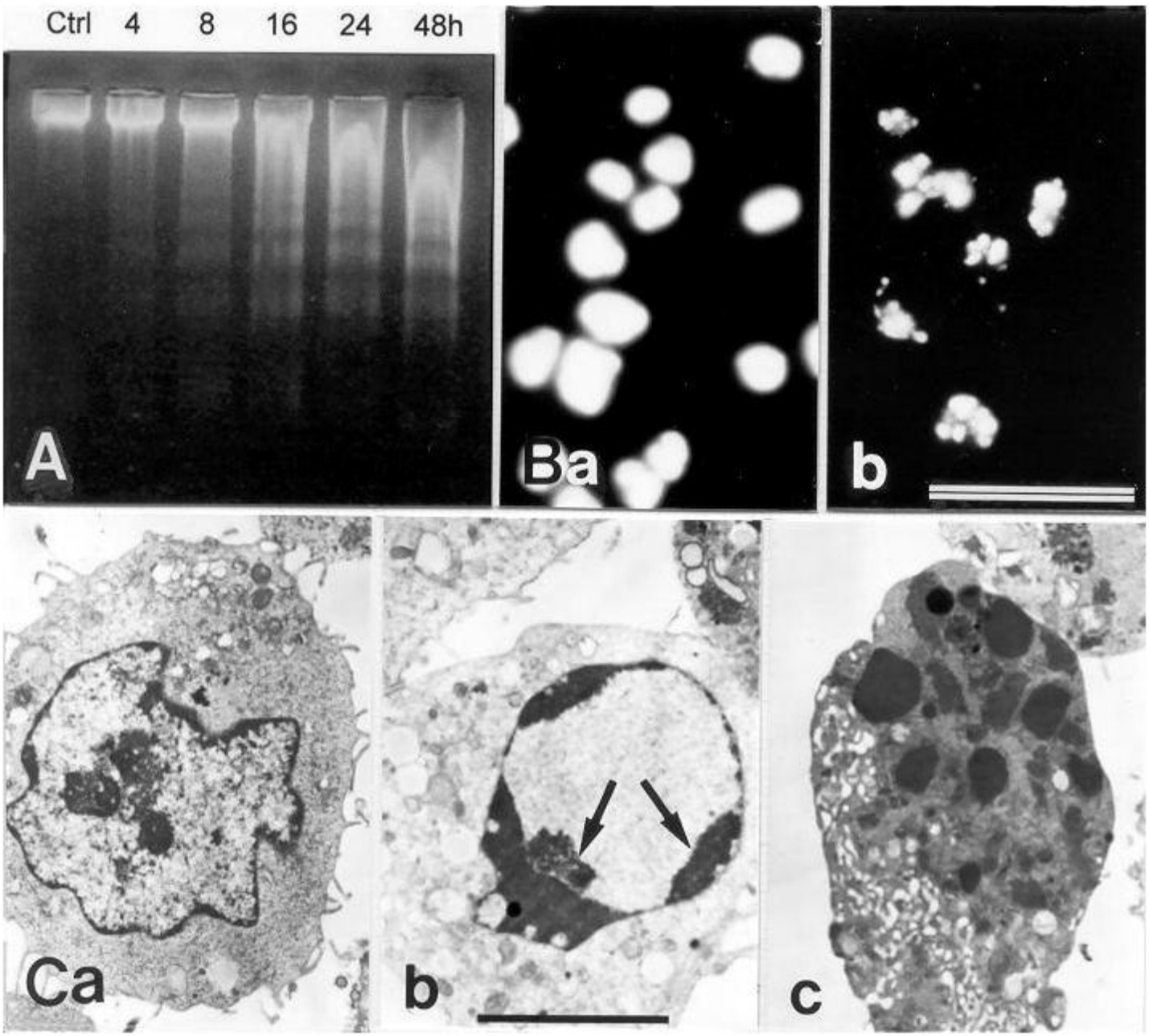

Fig.4

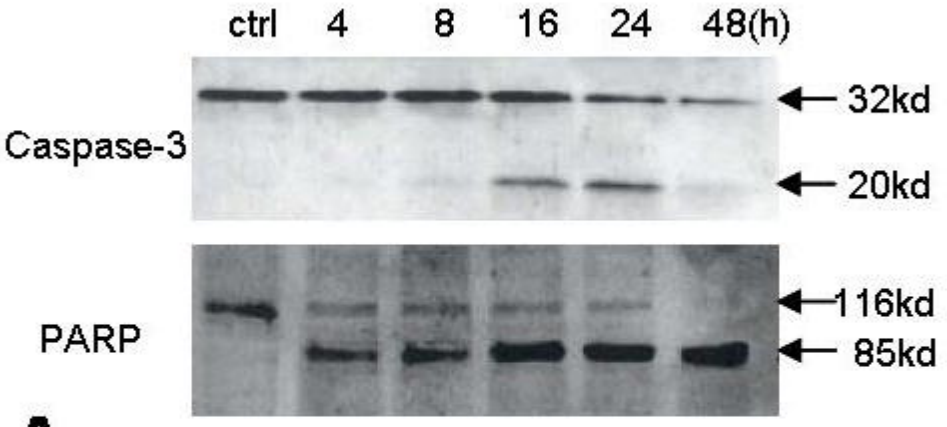
ctrl
4
8
16
24
48(h)
Caspase-3
32kd
20kd
PARP
116kd
85kd

A

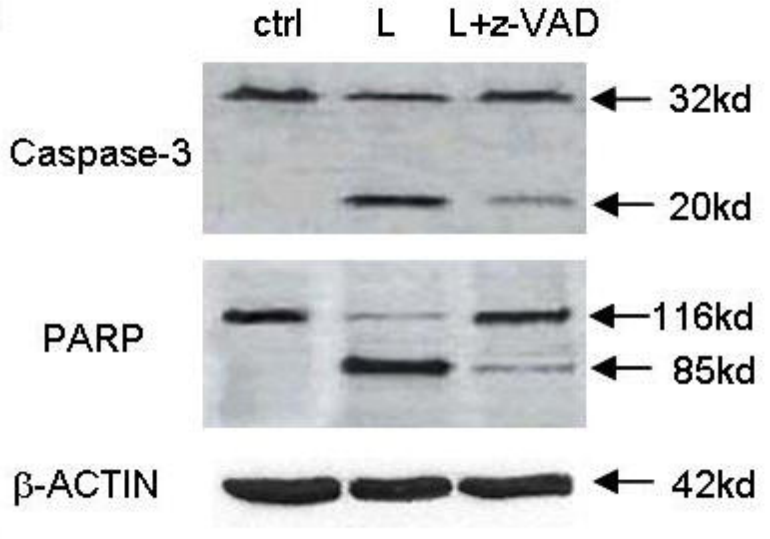
ctrl
L
L+z-VAD
Caspase-3
32kd
20kd
PARP
116kd
85kd
β-ACTIN
42kd

B

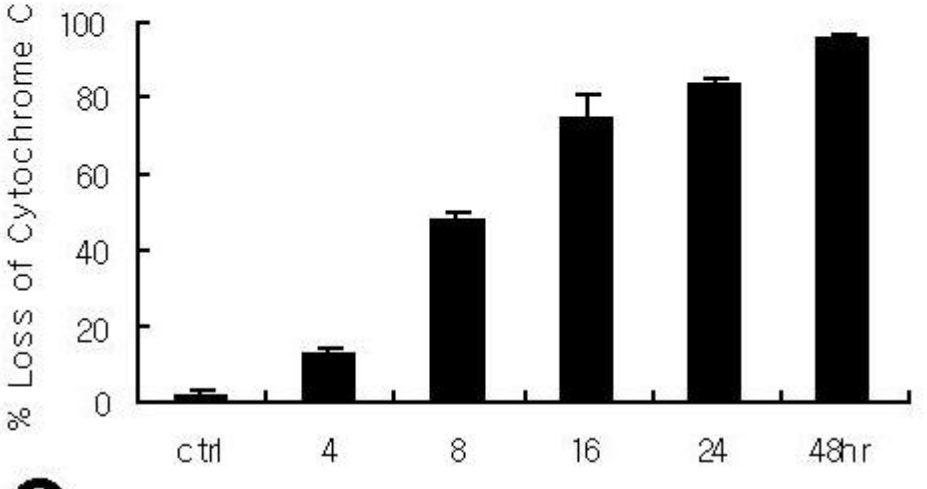
% Loss of Cytochrome C
100
80
60
40
20
0
ctrl
4
8
16
24
48hr

C

Fig.5

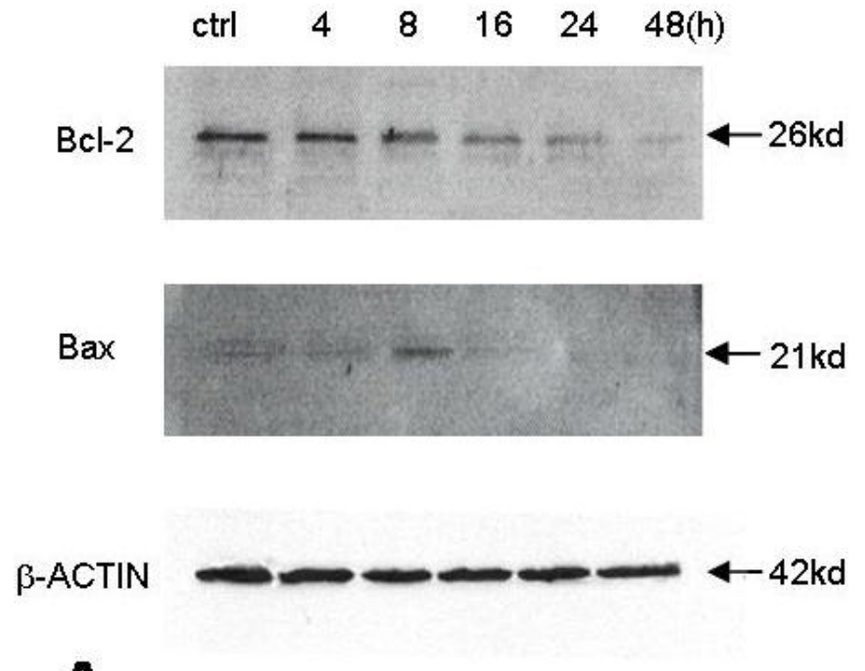
ctrl
4
8
16
24
48(h)
Bcl-2
26kd
Bax
21kd
β-ACTIN
42kd

A

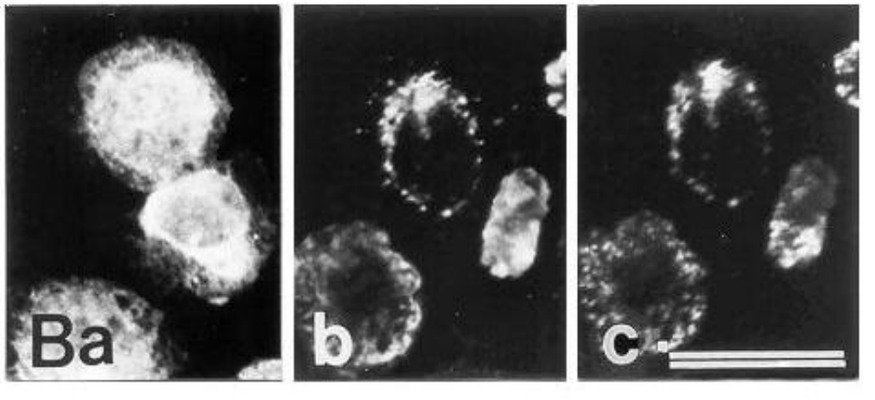
Ba
b
c

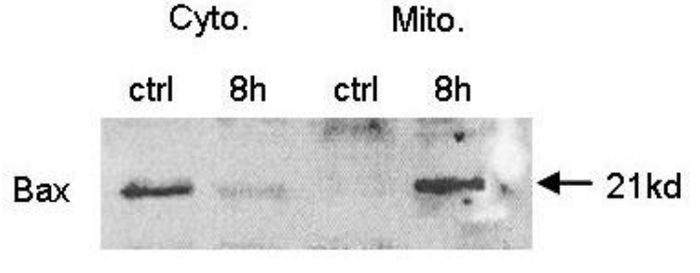
Cyto.
Mito.
ctrl
8h
ctrl
8h
Bax
21kd

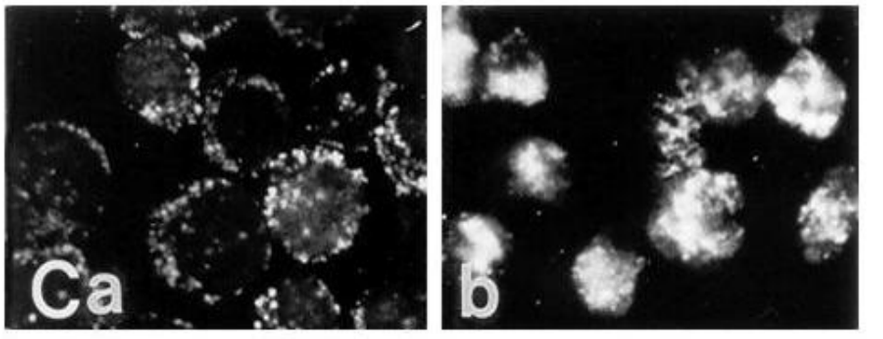
Ca
b

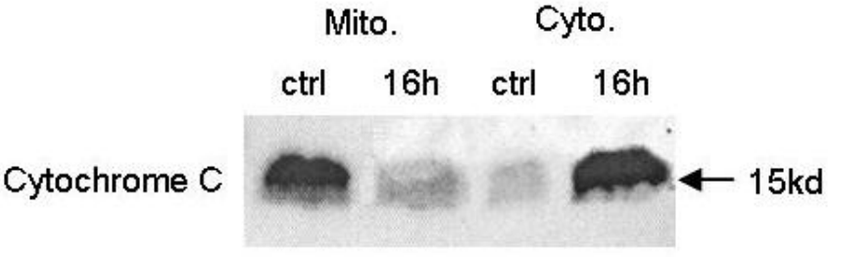
Mito.
Cyto.
ctrl
16h
ctrl
16h
Cytochrome C
15kd

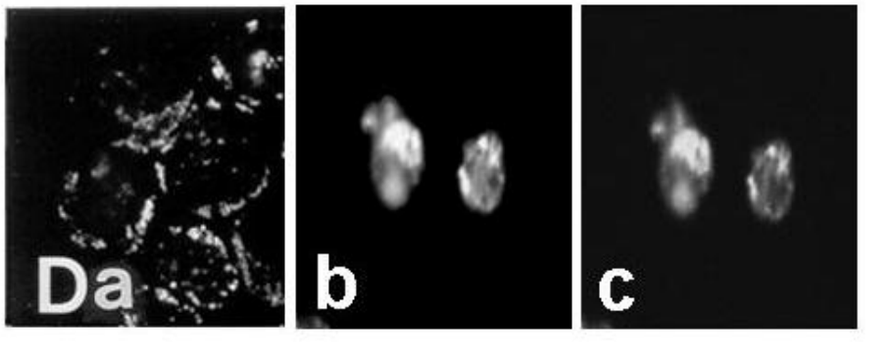
Da
b
c

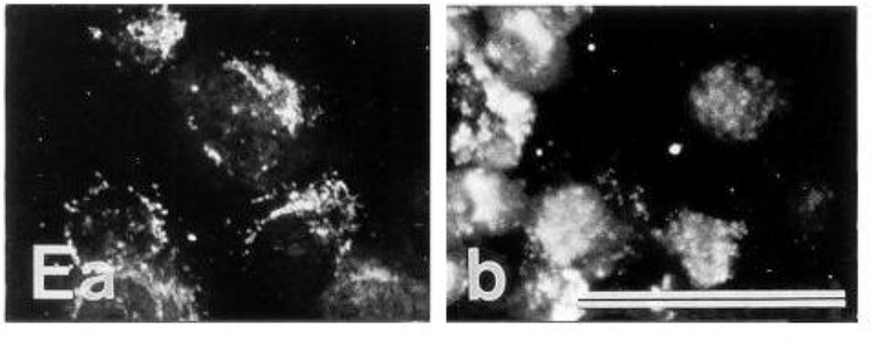
Ea
b

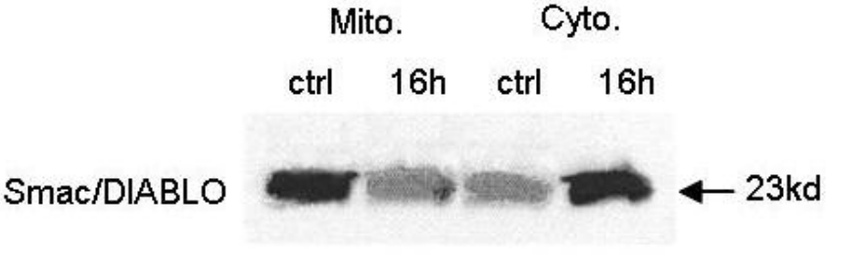
Mito.
Cyto.
ctrl
16h
ctrl
16h
Smac/DIABLO
23kd

Fig.6

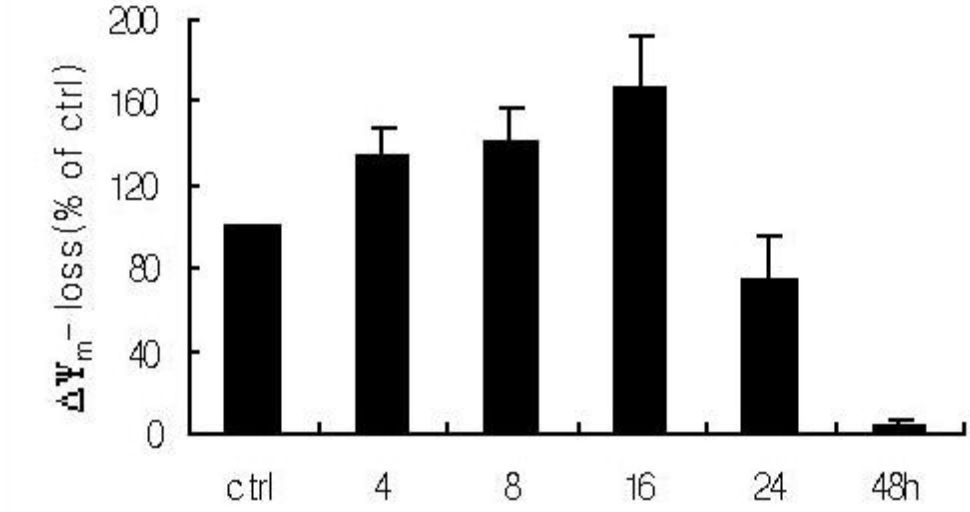
200
160
120
80
40
0
ΔΨm-loss(% of ctrl)
ctrl
4
8
16
24
48h

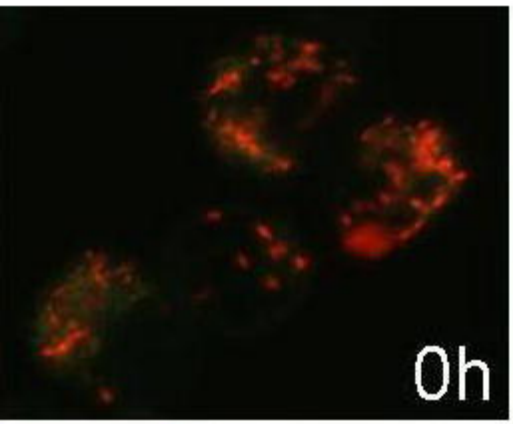
0h

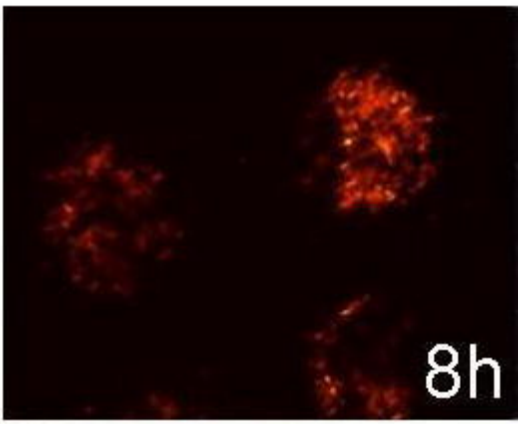
8h

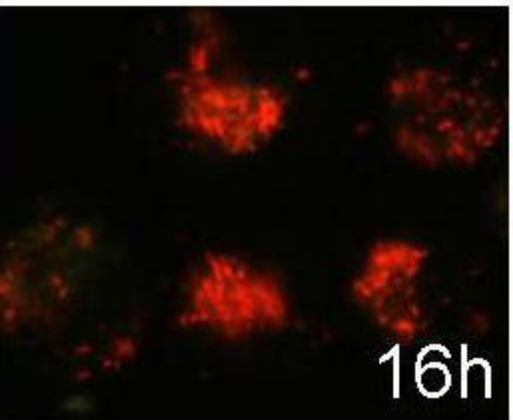
16h

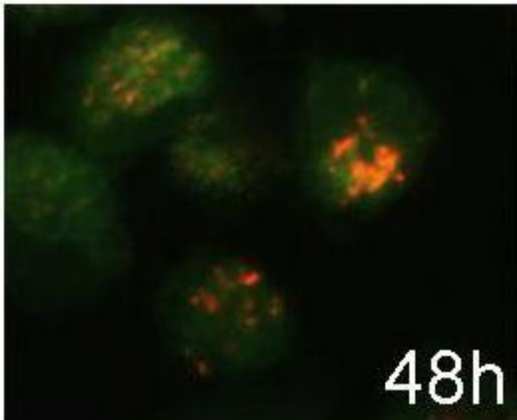
48h

Fig.7

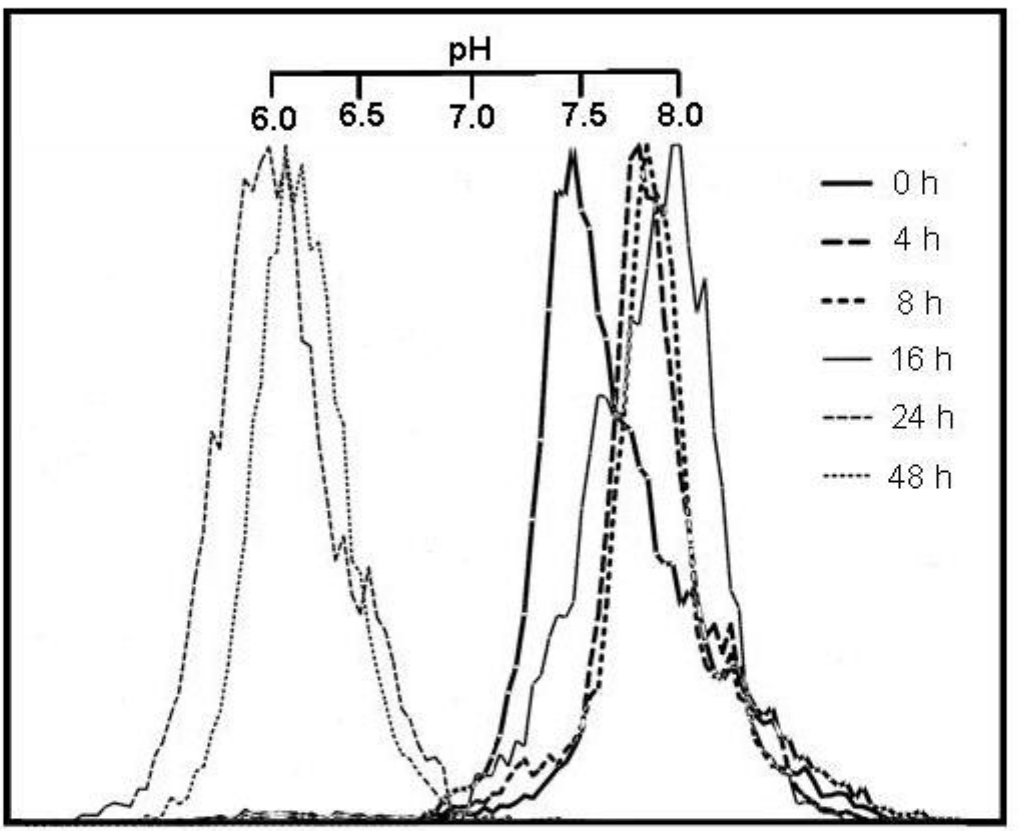
pH
6.0
6.5
7.0
7.5
8.0
0 h
4 h
8 h
16 h
24 h
48 h

A

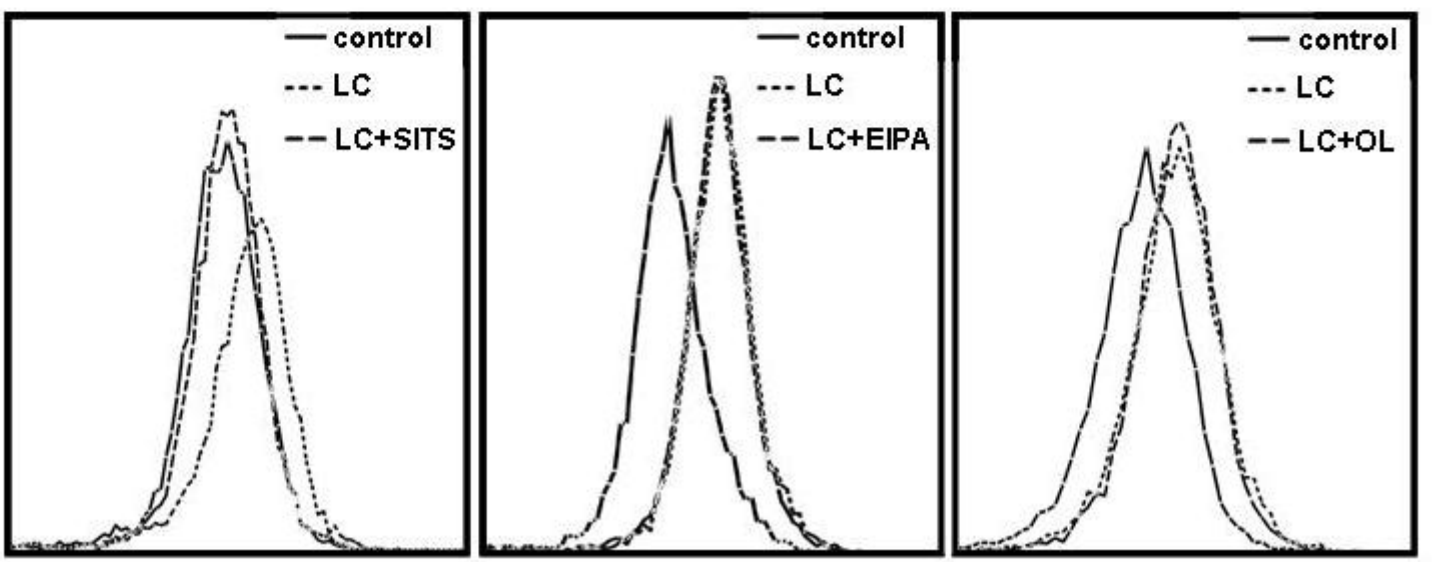
control
LC
LC+SITS
control
LC
LC+EIPA
control
LC
LC+OL

B

Fig.8

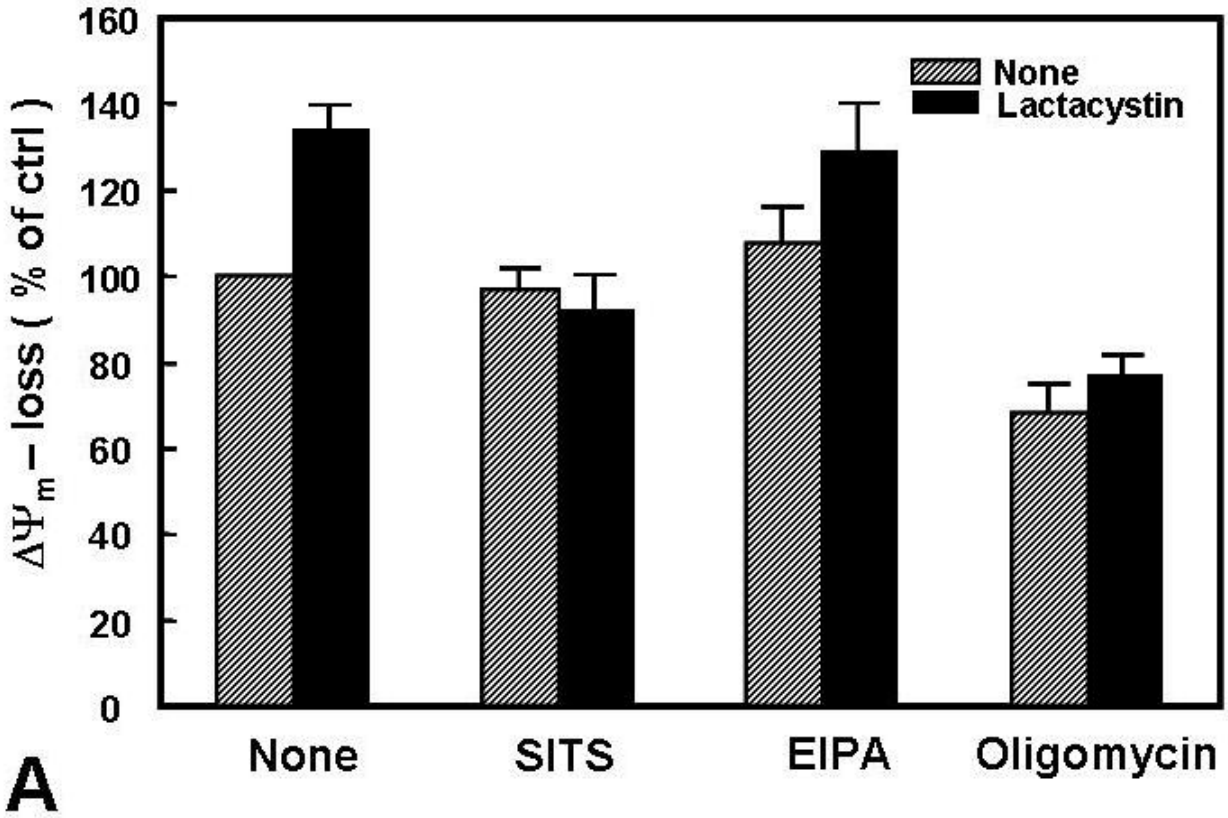
160
140
120
100
80
60
40
20
0
$\Delta\Psi_m$ – loss (% of ctrl)
None
Lactacystin
None
SITS
EIPA
Oligomycin
A

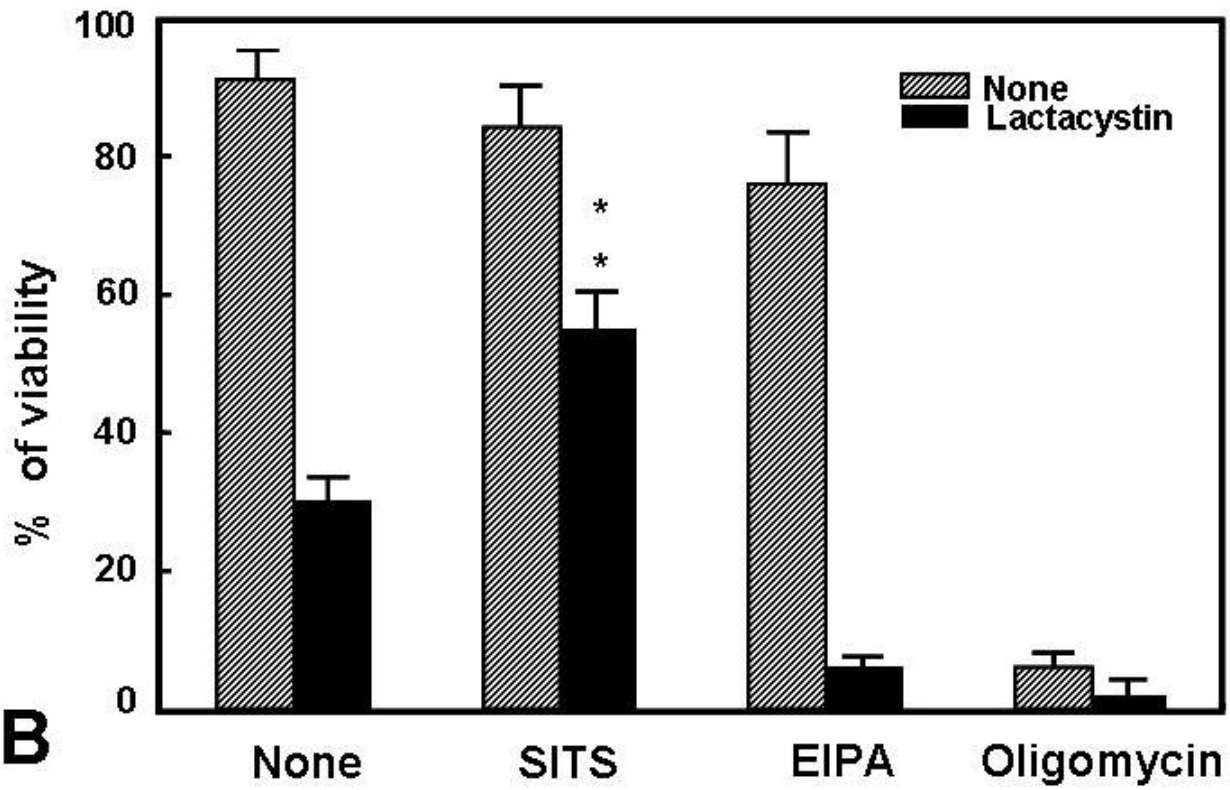
100
80
60
40
20
0
% of viability
None
Lactacystin
*
*
None
SITS
EIPA
Oligomycin
B